



HAL
open science

Diode-pumped mode-locked Yb:Sc₂SiO₅ laser generating 38 fs pulses

Lulu Dong, Zhang-Lang Lin, Pavel Loiko, Yichen Liu, Ge Zhang, Huang-Jun Zeng, Wen-Ze Xue, Shande Liu, Lihe Zheng, Liangbi Su, et al.

► **To cite this version:**

Lulu Dong, Zhang-Lang Lin, Pavel Loiko, Yichen Liu, Ge Zhang, et al.. Diode-pumped mode-locked Yb:Sc₂SiO₅ laser generating 38 fs pulses. *Optics Express*, 2023, 31 (8), pp.12463-12470. 10.1364/OE.486560 . hal-04209398

HAL Id: hal-04209398

<https://hal.science/hal-04209398>

Submitted on 2 Nov 2023

HAL is a multi-disciplinary open access archive for the deposit and dissemination of scientific research documents, whether they are published or not. The documents may come from teaching and research institutions in France or abroad, or from public or private research centers.

L'archive ouverte pluridisciplinaire **HAL**, est destinée au dépôt et à la diffusion de documents scientifiques de niveau recherche, publiés ou non, émanant des établissements d'enseignement et de recherche français ou étrangers, des laboratoires publics ou privés.

Diode-pumped mode-locked Yb:Sc₂SiO₅ laser generating 38 fs pulses

LULU DONG,¹ ZHANG-LANG LIN,² PAVEL LOIKO,³ YICHEN LIU,¹ GE ZHANG,² HUANG-JUN ZENG,² WEN-ZE XUE,² SHANDE LIU,⁴ LIHE ZHENG,⁵ LIANGBI SU,⁶ XAVIER MATEOS,⁷ HAIFENG LIN,⁸ VALENTIN PETROV,⁹ LI WANG,⁹ AND WEIDONG CHEN^{2,9,*}

¹School of Science, Qingdao University of Technology, 266525 Qingdao, China

²Fujian Institute of Research on the Structure of Matter, Chinese Academy of Sciences, 350002 Fuzhou, China

³Centre de Recherche sur les Ions, les Matériaux et la Photonique (CIMAP), UMR 6252 CEA-CNRS-ENSICAEN, Université de Caen, 6 Boulevard Maréchal Juin, 14050 Caen Cedex 4, France

⁴College of Electronic and Information Engineering, Shandong University of Science and Technology, 266590 Qingdao, China

⁵School of Physics and Astronomy, Yunnan University, 650091 Kunming, China

⁶State Key Laboratory of High Performance Ceramics and Superfine Microstructure, Shanghai Institute of Ceramics, Chinese Academy of Sciences, 201899 Shanghai, China

⁷Universitat Rovira i Virgili, URV, Física i Cristal·lografia de Materials, (FiCMA)- Marcel·lí Domingo I, 43007 Tarragona, Spain

⁸College of Physics and Optoelectronic Engineering, Shenzhen University, 518118 Shenzhen, China

⁹Max Born Institute for Nonlinear Optics and Short Pulse Spectroscopy, Max-Born-Str. 2a, 12489 Berlin, Germany

*chenweidong@fjirsm.ac.cn

Abstract: We report on sub-40 fs pulse generation from an Yb:Sc₂SiO₅ laser pumped by a spatially single-mode fiber-coupled laser diode at 976 nm. A maximum output power of 545 mW was obtained at 1062.6 nm in the continuous-wave regime, corresponding to a slope efficiency of 64% and a laser threshold of 143 mW. A continuous wavelength tuning across 80 nm (1030–1110 nm) was also achieved. Implementing a SESAM for starting and stabilizing the mode-locked operation, the Yb:Sc₂SiO₅ laser delivered soliton pulses as short as 38 fs at 1069.5 nm with an average output power of 76 mW at a pulse repetition rate of ~79.8 MHz. The maximum output power was scaled to 216 mW for slightly longer pulses of 42 fs, which corresponded to a peak power of 56.6 kW and an optical efficiency of 22.7%. To the best of our knowledge, these results represent the shortest pulses ever achieved with any Yb³⁺-doped rare-earth oxyorthosilicate crystal.

© 2023 Optical Society of America under the terms of the [OSA Open Access Publishing Agreement](#)

1. Introduction

Ytterbium (Yb³⁺) doped rare-earth oxyorthosilicates with a general chemical formula Yb³⁺:RE₂SiO₅ (where RE = Gd [1], Y [2], Lu [3], Sc [4] or their mixtures [5, 6]), crystallize in the monoclinic system (sp. gr. $C2/c - C_{2h}^6$). In the host lattice, Yb³⁺ ions can reside in two non-equivalent rare-earth sites of C₁ symmetry with VI- and VII-fold oxygen coordination and a strong distortion of the metal-ligand distances. This arrangement leads to strong crystal fields causing a relatively large Stark splitting of the ground (²F_{7/2}) manifold [7] of the Yb³⁺ ions favoring relatively long emission wavelengths, increased Stark bandwidths and low laser threshold with weak temperature sensitivity. Monoclinic rare-earth oxyorthosilicate crystals are optically biaxial (positive) and provide polarized emission spectra. As host matrices, they feature high thermal conductivities [8] favoring power scalable laser operation. Finally, the Yb³⁺:RE₂SiO₅ crystals can be grown by the Czochralski method.

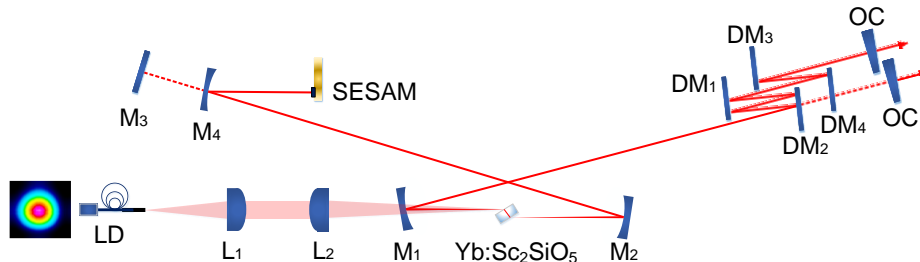
48 The broadband emission properties and good thermal behavior of $\text{Yb}^{3+}:\text{RE}_2\text{SiO}_5$ crystals
 49 make them extremely suitable for the development of high-power tunable and femtosecond
 50 lasers emitting in $\sim 1 \mu\text{m}$ spectral range when pumping by commercial InGaAs laser diodes at
 51 $\sim 980 \text{ nm}$ [9-11]. For reaching sub-100 fs pulse durations with the $\text{Yb}^{3+}:\text{RE}_2\text{SiO}_5$ crystals,
 52 usually, Kerr-lens mode-locking (KLM) is implemented. Using $\text{Yb}:\text{Gd}_2\text{SiO}_5$ as a gain medium,
 53 72 fs pulses were generated at 1050 nm via KLM corresponding to an average output power of
 54 85 mW [12]. Slightly shorter pulse duration could be obtained with “mixed” (solid-solution)
 55 crystals as gain media. Diode-pumped KLM lasers generating pulses as short as 61 fs and 55 fs
 56 were demonstrated with $\text{Yb}:(\text{Lu},\text{Y})_2\text{SiO}_5$ [13] and $\text{Yb}:(\text{Gd},\text{Y})_2\text{SiO}_5$ [14]. Even shorter pulse
 57 duration of 54 fs was obtained from a diode-pumped KLM $\text{Yb}:\text{Lu}_2\text{SiO}_5$ laser with a central
 58 wavelength of 1052 nm and an average output power of 25 mW [15].

59 One of the well-known representatives of the rare-earth oxyorthosilicate laser crystals is the
 60 Yb^{3+} -doped scandium oxyorthosilicate $\text{Yb}:\text{Sc}_2\text{SiO}_5$ (shortly $\text{Yb}:\text{SSO}$). It exhibits a relatively
 61 higher thermal conductivity of $7.5 \text{ Wm}^{-1}\text{K}^{-1}$ (average value, for 1 at.% Yb^{3+} doping) at room
 62 temperature compared to its isotopes and a negative thermo-optic coefficient of $-6.3 \times 10^{-6} \text{ K}^{-1}$
 63 [8], which ensures good heat removal and a relatively weak thermal lensing effect when
 64 pumping with commercial high-power InGaAs laser diodes for power scalable laser operation.
 65 Yb^{3+} ions in this material exhibit large Stark splitting of the ground ($^2\text{F}_{7/2}$) manifold (1027 cm^{-1}
 66 [8]), which is attractive for low laser threshold laser operation. In addition, they show relative
 67 broad absorption zero-phonon line (ZPL) with a full width at half maximum (FWHM) of 24 nm
 68 at 976 nm, which releases the requirements for wavelength stabilization for high-power InGaAs
 69 laser diodes [8]. The broadband gain profiles and the moderate luminescence lifetime (0.7 ms)
 70 of Yb^{3+} ions in the Sc_2SiO_5 crystal make it very suitable for application in femtosecond regime,
 71 both in oscillators and amplifiers [4, 16-18]. Power scalable operation in the femtosecond time
 72 domain would also be possible with the thin-disk configuration. A thin-disk $\text{Yb}:\text{Sc}_2\text{SiO}_5$ laser
 73 mode-locked (ML) with a Semiconductor Saturable Absorber Mirror (SESAM) delivered a
 74 maximum average output power of 27.8 W with a pulse duration of 298 fs at 1036 nm [19].

75 In the present work, we explore the potential for sub-40 fs pulse generation from SESAM
 76 ML $\text{Yb}:\text{Sc}_2\text{SiO}_5$ lasers pumped by a spatially single-mode fiber-coupled InGaAs laser diode.

77 2. Laser set-up

78 An X-shaped astigmatically compensated linear cavity was used, see Fig. 1. A rectangular laser
 79 element was cut from the as-grown 4.4 at.% Yb^{3+} -doped Sc_2SiO_5 crystal (actual composition)
 80 grown by the Czochralski method [20-23] and oriented for light propagation along the optical
 81 indicatrix axis Y (Y -cut). It had an aperture of $3.3 \text{ mm} \times 3.3 \text{ mm}$ and a thickness of 3 mm. This
 82 orientation was selected to benefit from high pump absorption efficiency under ZPL pumping.
 83 The laser element was mounted in a passively cooled copper holder using Indium foil for better
 84 heat removal and placed at Brewster’s angle for $\text{E} \parallel \text{X}$ polarization between two concave
 85 dichroic folding mirrors M_1 and M_2 (radius of curvature: $\text{RoC} = -100 \text{ mm}$).



86
 87 **Fig. 1.** Experimental layout of the $\text{Yb}:\text{Sc}_2\text{SiO}_5$ laser. LD: fiber-coupled laser diode at 976 nm;
 88 L_1 : aspherical collimating lens; L_2 : spherical focusing lens; M_1 , M_2 and M_4 : concave mirrors
 89 ($\text{RoC} = -100 \text{ mm}$); M_3 : flat end mirror; $\text{DM}_1 - \text{DM}_4$: flat dispersive mirrors; OC: output coupler.
 90 *Inset* – spatial profile of the pump radiation at full pump power.

91 The pump source was a spatially single-mode, fiber-coupled InGaAs laser diode emitting
 92 unpolarized radiation at 976 nm. Its emission wavelength was locked using a Fiber Bragg
 93 grating (FBG) leading to a spectral linewidth (FWHM) of 0.2 nm. The pump beam was nearly
 94 diffraction-limited with a measured M^2 factor of ~ 1.02 . The pump radiation was collimated
 95 using an aspherical lens L_1 (focal length: $f = 25.4$ mm) and then focused into the laser crystal
 96 through the M_1 mirror with a spherical focusing lens L_2 ($f = 75$ mm) resulting in a beam waist
 97 radius of $14 \mu\text{m} \times 29 \mu\text{m}$ in the sagittal and tangential planes, respectively.

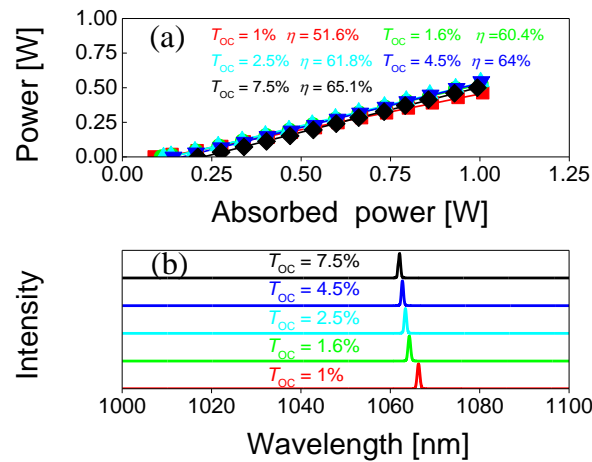
98 For continuous-wave (CW) laser operation, a four-mirror cavity was employed without a
 99 saturable absorber. One cavity arm was terminated by a flat end mirror M_3 and the other
 100 arm – by a plane-wedged output coupler (OC) with a transmission at the laser wavelength T_{OC}
 101 ranging from 1% to 7.5%. The cavity mode inside the laser cavity was simulated using the ray
 102 transfer matrix formalism yielding a waist radius in the laser crystal of $20 \mu\text{m} \times 40 \mu\text{m}$ in the
 103 sagittal and tangential planes, respectively. **The measured single-pass pump absorption under**
 104 **lasing conditions only slightly decreased with T_{OC} in the CW regime, from 72.8% to 71.7%.**

105 For ML operation, the flat end mirror M_3 was substituted by a curved mirror M_4 (RoC = -
 106 100 mm) and the cavity arm was terminated by a commercial SESAM (BATOP, GmbH) with
 107 a modulation depth of $\sim 0.6\%$ at a central wavelength of 1040 nm (high reflection band:
 108 1000 – 1070 nm), a non-saturable loss of $\sim 0.4\%$, a saturation fluence of $70 \mu\text{J}/\text{cm}^2$, and a
 109 relaxation time of ~ 1 ps. The intracavity group delay dispersion (GDD) was managed by
 110 implementing four flat dispersive mirrors (DMs) characterized by a GDD per bounce of
 111 $\text{DM}_1 = \text{DM}_2 = -150 \text{ fs}^2$ and $\text{DM}_3 = \text{DM}_4 = -100 \text{ fs}^2$. The resulting total round-trip negative
 112 GDD amounted to -1600 fs^2 to compensate for the material dispersion and to balance the self-
 113 phase modulation (SPM) induced by the Kerr nonlinearity of the laser crystal. The physical
 114 length of the ML laser cavity was 1.88 m which corresponds to a pulse repetition rate of
 115 ~ 79.8 MHz.

116 3. Results and discussion

117 3.1 Continuous-wave laser operation

118 The Yb:Sc₂SiO₅ laser generated a maximum output power of 545 mW at 1062.6 nm with a
 119 slope efficiency η of 64% (vs. absorbed pump power using $T_{OC} = 4.5\%$, see Fig. 2(a).

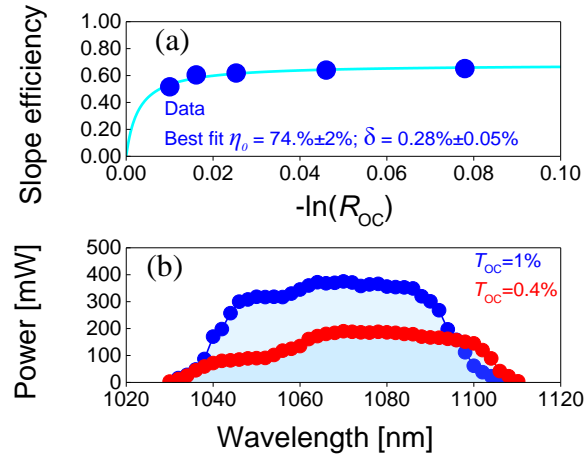


120
 121 **Fig. 2.** CW Yb:Sc₂SiO₅ laser: (a) Input - output dependences for different OCs, η – slope
 122 efficiency; (b) Typical spectra of laser emission (laser polarization: $E \parallel X$).

123 This corresponded to an absorbed pump power of 1.0 W and an optical efficiency of 54.5%.
 124 The laser threshold was 143 mW for this OC. The laser polarization was linear ($E \parallel X$). Even
 125 higher η of 65.1% was obtained with a higher $T_{OC} = 7.5\%$ reaching an output power of 500 mW
 126 at 1062 nm at an absorbed power of 0.99 W. The laser threshold increased with the output

127 coupling, from 89 mW ($T_{OC} = 1\%$) to 211 mW ($T_{OC} = 7.5\%$). The laser wavelength in the CW
 128 regime experienced a slight blue-shift with increasing the OC transmission, from 1066 to
 129 1062 nm, as shown in Fig. 2(c). This behavior is typical for quasi-three-level Yb lasers with
 130 inherent reabsorption at the laser wavelength and agrees with the gain spectra of Yb^{3+} ions in
 131 the Sc_2SiO_5 crystal.

132 The Caird analysis was applied to determine the passive losses in the Yb: $\text{Yb}:\text{Sc}_2\text{SiO}_5$
 133 crystal: the measured laser slope efficiency was fitted as a function of $-\ln(R_{OC})$, where
 134 $R_{OC} = 1 - T_{OC}$ is the output coupler reflectivity [20]. The analysis yielded the total round-trip
 135 cavity losses of $\delta = 0.28 \pm 0.05\%$ (reabsorption losses excluded) and an intrinsic slope
 136 efficiency η_0 of $74.4 \pm 2\%$, as shown in Fig. 3(a).



137

138 **Fig. 3.** CW Yb:Sc₂SiO₅ laser: (a) Caird analysis: laser slope efficiency plotted vs. $-\ln(R_{OC})$;
 139 where $R_{OC} = 1 - T_{OC}$; (b) Laser tuning curves obtained with a Lyot filter, $T_{OC} = 0.4\%$ and 1% .

140 The potential of the Yb:Sc₂SiO₅ crystal for broadband wavelength tuning was studied in the
 141 CW regime by inserting a Lyot filter (a 2-mm thick quartz plate) at Brewster's angle close to
 142 the OC. The laser wavelength was continuously tunable between 1032 - 1106 nm, i.e., across
 143 74 nm at the zero-power-level, for $T_{OC} = 1\%$ at an incident pump power of 1.5 W. For smaller
 144 $T_{OC} = 0.4\%$ at an incident pump power of 1.38 W, the tuning range was broader, 80 nm
 145 (1030 - 1110 nm), see Fig. 3(b). In this case, the power maximum of the tuning curve was
 146 observed at ~1070 nm.

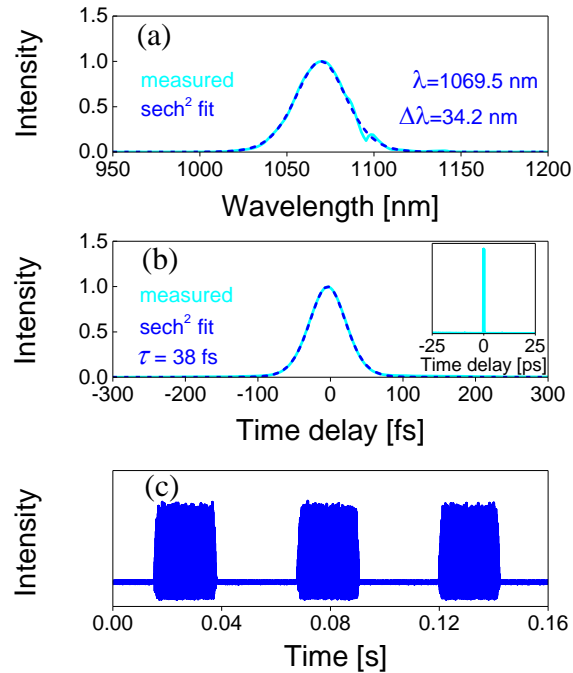
147 The broadband tuning properties of Yb:Sc₂SiO₅ are due to the strong crystal-fields for the
 148 dopant Yb^{3+} ions in low-symmetry (C_1) sites in this crystal leading to a large total Stark splitting
 149 of the ground-state multiplet ($^2F_{7/2}$), namely 770 cm^{-1} (site I) and 1026 cm^{-1} (site II) [4]. Another
 150 reason is the spectral broadening due to the electron-phonon interaction.

151 3.2 Mode-locked laser operation

152 By implementing a commercial SESAM and four flat DMs into the laser cavity resulting in a
 153 total round-trip negative GDD of -1600 fs^2 , stable and self-starting ML operation was readily
 154 achieved. The shortest pulses were obtained with a 1.6% OC. Their characterization is shown
 155 in Fig. 4.

156 The Yb:Sc₂SiO₅ laser delivered soliton pulses with an emission spectral bandwidth
 157 (FWHM) of 34.2 nm at a central wavelength of 1069.5 nm by assuming a sech²-shape spectral
 158 intensity profile, see Fig. 4(a). The dip in the laser spectrum at ~1095 nm originates from the
 159 spectral profile of reflectivity of the used SESAM. The recorded second-harmonic generation
 160 (SHG) based intensity autocorrelation trace gave a deconvolved pulse duration of 38 fs
 161 (FWHM) assuming a sech²-shaped temporal pulse profile, see Fig. 4(b). The corresponding
 162 time-bandwidth product (TBP) of 0.341 was slightly above the Fourier-transform-limit (0.315).

163 A long-scale (50 ps) background-free intensity autocorrelation scan confirmed the single-pulse
 164 steady-state mode-locking, see the inset in Fig. 4(b). Under these conditions, an average output
 165 power of 76 mW was obtained at an absorbed pump power of 1.02 W (1.385 W incident pump
 166 power), corresponding to an optical efficiency of 7.5% and a peak power of 22.1 kW.
 167 To emphasize the self-starting nature of mode-locking, a chopper rotating at a frequency of
 168 20 Hz was inserted into the cavity and a fast photodetector was used to monitor the ML pulse
 169 train, see Fig. 4(c). The result well illustrates that the Yb:Sc₂SiO₅ laser was self-starting into a
 170 steady ML operation without any external perturbation.



171
 172 **Fig. 4.** SESAM ML Yb:Sc₂SiO₅ laser with $T_{OC} = 1.6\%$. (a) Optical spectrum; (b) SHG-based
 173 intensity autocorrelation trace, *dashed curve* - sech² fit. *Inset:* intensity autocorrelation trace
 174 measured on a time span of 50 ps; (c) Oscilloscope trace of the shortest pulse train measured
 175 with a 20-Hz chopper inserted into the intracavity beam, illustrating the self-starting operation.

176 A radio-frequency (RF) spectrum analyzer was used for confirming the stability of the ML
 177 operation for the shortest pulses. A relatively high extinction ratio of >71 dBc above the noise
 178 level for the fundamental beat note at 79.81 MHz in combination with the uniform harmonics
 179 recorded on a 1-GHz frequency span provided evidence of highly stable CW-ML operation
 180 without any Q-switching or multi-pulsing instabilities, see Fig. 5.

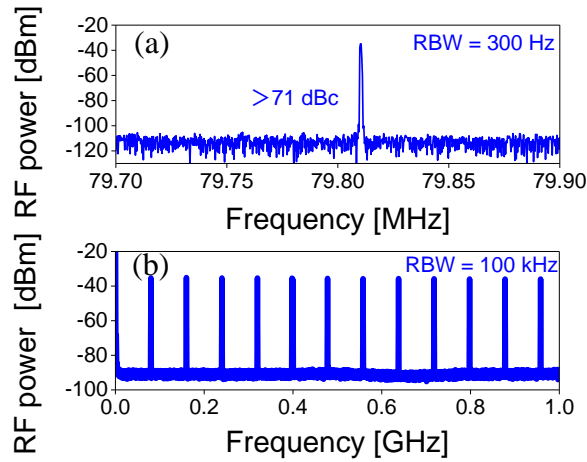


Fig. 5. RF spectra of the ML Yb:Sc₂SiO₅ laser with $T_{OC} = 1.6\%$: (a) Fundamental beat note at 79.81 MHz recorded with a resolution bandwidth (RBW) of 300 Hz, and (b) harmonics on a 1-GHz frequency span recorded with a RBW of 100 kHz.

181
182
183
184

185 An IR camera was placed at 0.8 m away from the OC to record the far-field beam profiles
186 both in the CW and ML regimes to reveal the dominating ML mechanism for generating the
187 shortest pulse duration. The transition from CW to ML regime was accompanied by a slight
188 shrinking of the beam size (diameter) from $1.50 (x) \times 1.69 (y) \text{ mm}^2$ to $1.51 (x) \times 1.56 (y) \text{ mm}^2$,
189 as shown in Fig. 6. Such observation validated the underlying ML mechanism dominated by
190 Kerr-lens mode-locking stabilized by the SESAM, which is supported by the high-brightness
191 of the pump laser. However, the pulse shaping by the SESAM cannot be ruled out in view of
192 the much wider stability zone and the self-starting mode-locking operation. Such a hybrid pulse
193 shaping mechanism introduced an enhanced self-amplitude modulation (SAM) by the Kerr-
194 lens effect, which assisted the SESAM ML operation for shorter pulse duration, i.e., Kerr-lens
195 assisted SESAM ML operation.

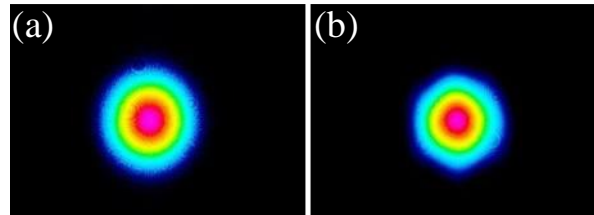


Fig. 6. Measured far-field beam profiles of the Yb:Sc₂SiO₅ laser ($T_{OC} = 1.6\%$): (a) CW and (b) ML regimes of operation.

196
197
198

199 The scaling of the average output power from the ML laser was achieved by employing
200 higher output coupling ($T_{OC} = 4\%$) while the pulse duration was optimized by the total round-
201 trip negative GDD of -1600 fs^2 . The maximum average output power amounted to 216 mW
202 (peak power 59.02 kW) for an absorbed pump power of 0.95 W (1.385 W incident pump
203 power). The optical spectrum of ML laser was centered at 1068.1 nm with a sech²-fitted spectral
204 FWHM of 29.5 nm. Pulses as short as 42 fs were obtained as confirmed by the measured SHG-
205 based autocorrelation trace. The corresponding TBP was 0.326 still being close to the Fourier-
206 transform-limit. The pulse repetition rate was $\sim 79.83 \text{ MHz}$ and the optical efficiency reached
207 22.7%.

208 4. Conclusion

209 To conclude, we report on sub-40 fs pulse generation from a passively mode-locked ytterbium
210 scandium oxyorthosilicate (Yb:Sc₂SiO₅) laser pumped by a spatially single-mode fiber-coupled

211 laser diode at 976 nm. Implementing a SESAM for starting and stabilizing the mode-locked
212 operation, the Yb:Sc₂SiO₅ laser delivered soliton pulses as short as 38 fs at 1069.5 nm with an
213 average output power of 76 mW and a pulse repetition rate of ~79.8 MHz, representing the
214 shortest pulses ever achieved with any Yb³⁺-doped rare-earth oxyorthosilicate crystals RE₂SiO₅
215 (parent or “mixed”). The mode-locking was self-starting. We suggest a hybrid pulse shaping
216 mechanism with an enhanced self-amplitude modulation introduced by the Kerr-lens effect,
217 which assisted the SESAM mode-locked operation resulting in a shorter pulse duration. Our
218 results indicate the potential of the Yb:Sc₂SiO₅ crystal for Kerr-lens mode-locked lasers.

219 **Funding.** National Natural Science Foundation of China (61975208, 62205171, 61905247, U21A20508); Sino-
220 German Scientist Cooperation and Exchanges Mobility Program (M-0040); National Key Research and Development
221 Program of China (2021YFB3601504); Grant PID2019-108543RB-I00 funded by MCIN/AEI/10.13
222 039/501100011033.

223 **Acknowledgment.** Xavier Mateos acknowledges the Serra Hünter program.

224 **Disclosures.** The authors declare no conflicts of interest.

225 **Data availability.** Data underlying the results presented in this paper are not publicly available at this time but may
226 be obtained from the authors upon reasonable request.

227 References

- 228 1. C. Yan, G. Zhao, L. Zhang, J. Xu, X. Liang, D. Juan, W. Li, H. Pan, L. Ding, and H. Zeng, "A new Yb-doped
229 oxyorthosilicate laser crystal: Yb:Gd₂SiO₅," *Solid State Commun.* **137**(8), 451 - 455 (2006).
- 230 2. M. Jacquemet, C. Jacquemet, N. Janel, F. Druon, F. Balembois, P. Georges, J. Petit, B. Viana, D. Vivien, and
231 B. Ferrand, "Efficient laser action of Yb:LSO and Yb:YSO oxyorthosilicates crystals under high-power diode-
232 pumping," *Appl. Phys. B* **80**(2), 171 - 176 (2005).
- 233 3. G. Toci, A. Pirri, A. Beitlerova, Y. Shoji, A. Yoshikawa, J. Hybler, M. Nikl, and M. Vannini, "Characterization
234 of the lasing properties of a 5% Yb doped Lu₂SiO₅ crystal along its three principal dielectric axes," *Opt. Express*
235 **23**(10), 13210 - 13221 (2015).
- 236 4. R. Gaume, B. Viana, J. Derouet, and D. Vivien, "Spectroscopic properties of Yb-doped scandium based
237 compounds Yb:CaSc₂O₄, Yb:SrSc₂O₄ and Yb:Sc₂SiO₅," *Opt. Mater.* **22**(2), 107 - 115 (2003).
- 238 5. J. Du, X. Liang, Y. Xu, R. Li, Z. Xu, C. Yan, G. Zhao, L. Su, and J. Xu, "Tunable and efficient diode-pumped
239 Yb³⁺:GYSO laser," *Opt. Express* **14**(8), 3333 - 3338 (2006).
- 240 6. W. Li, S. Xu, H. Pan, L. E. Ding, H. Zeng, W. Lu, C. Guo, G. Zhao, C. Yan, and L. Su, "Efficient tunable
241 diode-pumped Yb:LYSO laser," *Opt. Express* **14**(15), 6681 - 6686 (2006).
- 242 7. R. Gaume, P. Haumesser, B. Viana, D. Vivien, B. Ferrand, and G. Aka, "Optical and laser properties of
243 Yb:Y₂SiO₅ single crystals and discussion of the figure of merit relevant to compare ytterbium-doped laser
244 materials," *Opt. Mater.* **19**(1), 81 - 88 (2002).
- 245 8. L. Zheng, J. Xu, G. Zhao, L. Su, F. Wu, and X. Liang, "Bulk crystal growth and efficient diode-pumped laser
246 performance of Yb³⁺:Sc₂SiO₅," *Appl. Phys. B* **91**(3), 443 - 445 (2008).
- 247 9. W. L. Tian, J. F. Zhu, Y. N. Peng, Z. H. Wang, L. H. Zheng, L. B. Su, J. Xu, and Z. Y. Wei, "High power sub
248 100-fs Kerr-lens mode-locked Yb:YSO laser pumped by single-mode fiber laser," *Opt. Express* **26**(5), 5962 -
249 5969 (2018).
- 250 10. F. Thibault, D. Pelenc, F. Druon, Y. Zaouter, M. Jacquemet, and P. Georges, "Efficient diode-pumped
251 Yb³⁺:Y₂SiO₅ and Yb³⁺:Lu₂SiO₅ high-power femtosecond laser operation," *Opt. Lett.* **31**(10), 1555 - 1557
252 (2006).
- 253 11. W. Tian, Z. Wang, J. Zhu, L. Zheng, J. Xu, and Z. Wei, "Highly efficient and high-power diode-pumped
254 femtosecond Yb:LYSO laser," *Laser Phys. Lett.* **14**(4), 045802 (2017).
- 255 12. W. Tian, Z. Wang, J. Zhu, L. Zheng, X. Xu, J. Xu, and Z. Wei, "Diode-pumped Kerr-lens mode-locked
256 Yb:GSO laser generating 72 fs pulses," *Opt. Laser Technol.* **79**, 137 - 140 (2016).
- 257 13. W. L. Tian, Z. H. Wang, L. Wei, Y. N. Peng, J. W. Zhang, Z. Zhu, J. F. Zhu, H. N. Han, Y. L. Jia, L. H. Zheng,
258 J. Xu, and Z. Y. Wei, "Diode-pumped Kerr-lens mode-locked Yb:LYSO laser with 61 fs pulse duration," *Opt.*
259 *Express* **22**(16), 19040 - 19046 (2014).
- 260 14. J. Zhu, Z. Gao, W. Tian, J. Wang, Z. Wang, Z. Wei, L. Zheng, L. Su, and J. Xu, "Kerr-lens mode-locked
261 femtosecond Yb:GdYSiO₅ laser directly pumped by a laser diode," *Appl. Sci.* **5**(4), 817 - 824 (2015).
- 262 15. W. Tian, Z. Wang, J. Zhu, Z. Wei, L. Zheng, X. Xu, and J. Xu, "Generation of 54 fs laser pulses from a diode
263 pumped Kerr-lens mode-locked Yb:LSO laser," *Chin. Phys. Lett.* **32**(2), 024206 (2015).
- 264 16. W. Tan, D. Tang, J. Zhang, D. Shen, X. Xu, and J. Xu, "Dissipative soliton operation of an Yb³⁺:Sc₂SiO₅ laser
265 in the vicinity of zero group velocity dispersion," *Opt. Photon. Lett.* **5**(1), 1250001 (2012).
- 266 17. F. Pirzio, E. Caracciolo, M. Kemnitz, A. Guandalini, F. Kienle, J. Aus der Au, and A. Agnesi, "Performance
267 of Yb:Sc₂SiO₅ crystal in diode-pumped femtosecond oscillator and regenerative amplifier," *Opt. Express*
268 **23**(10), 13115 - 13120 (2015).

- 269
270
271
272
273
274
275
276
277
278
279
280
281
282
283
18. C. Xu, D. Tang, J. Zhang, H. Zhu, X. Xu, L. Zheng, L. Su, and J. Xu, "Sub-100 fs pulse generation in a diode pumped Yb:Sc₂SiO₅ laser," *Opt. Commun.* **294**, 237 - 240 (2013).
 19. K. S. Wentsch, L. Zheng, J. Xu, M. A. Ahmed, and T. Graf, "Passively mode-locked Yb³⁺:Sc₂SiO₅ thin-disk laser," *Opt. Lett.* **37**(22), 4750 - 4752 (2012).
 20. Z. Zou, L. Zheng, J. Wang, D. Jiang, S. Liu, Q. Sai, J. Wang, H. Hu, and L. Su, "Crystal growth and photoluminescence spectra properties of (Yb_xNd_ySc_{1-x-y})₂SiO₅ laser crystal," *Laser Phys. Lett.* **15**(8), 085703 (2018).
 21. Y. Zhao, Q. Wang, L. Meng, Y. Yao, S. Liu, N. Cui, L. Su, L. Zheng, H. Zhang, and Y. Zhang, "Anisotropy of the thermal and laser output properties in Yb,Nd:Sc₂SiO₅ crystal," *Chin. Opt. Lett.* **19**(4), 041405 (2021).
 22. X. Liu, J. Guo, L. Zheng, J. Liu, Q. Peng, Y. Ge, and J. Xu, "Two - dimensional graphdiyne for passively Q-switched Yb³⁺:Sc₂SiO₅ laser," *Microw. Opt. Technol. Lett.* **63**(9), 2292 - 2296 (2021).
 23. L. Dong, Y. Yao, Q. Wang, S. Liu, L. Zheng, Y. Xu, D. Li, H. Zhang, Z. Zou, and L. Su, "Tunable and mode-locking Yb, Nd:Sc₂SiO₅ femtosecond laser," *IEEE Photon. Technol. Lett.* **30**(24), 2167 - 2170 (2018).
 24. J. A. Caird, S. A. Payne, P. R. Staver, A. Ramponi, and L. Chase, "Quantum electronic properties of the Na₃Ga₂Li₃F₁₂:Cr³⁺ laser," *IEEE J. Quantum Electron.* **24**(6), 1077 - 1099 (1988).